Drug Resistance Updates 75 (2024) 101087

Contents lists available at ScienceDirect

Drug Resistance Updates

journal homepage: www.elsevier.com/locate/drup

Heterogeneity of SOS response expression in clinical isolates of *Escherichia coli* influences adaptation to antimicrobial stress

Sara Diaz-Diaz [a,*], Andrea Garcia-Montaner [b], Roberta Vanni [b], Marina Murillo-Torres [a,b], Esther Recacha [a,c,d], Marina R. Pulido [a,b,d], Maria Romero-Muñoz [b], Fernando Docobo-Pérez [a,b,d], Alvaro Pascual [a,b,c,d], Jose Manuel Rodriguez-Martinez [a,b,d]

[a] Instituto de Biomedicina de Sevilla (IBiS), Hospital Universitario Virgen Macarena/CSIC/Universidad de Sevilla, Sevilla, Spain, Sevilla, Spain
[b] Departamento de Microbiología, Facultad de Medicina, Universidad de Sevilla, Sevilla, Spain
[c] Unidad Clínica de Enfermedades Infecciosas y Microbiología, Hospital Universitario Virgen Macarena, Sevilla, Spain
[d] Centro de Investigación Biomédica en Red en Enfermedades Infecciosas (CIBERINFEC), Instituto de Salud Carlos III, Madrid, Spain

ARTICLE INFO

Keywords:
Heterogeneity of gene expression
Clinical isolates
Antimicrobial stress
Quinolones
recA gene
SOS response

ABSTRACT

In recent years, new evidence has shown that the SOS response plays an important role in the response to antimicrobials, with involvement in the generation of clinical resistance. Here we evaluate the impact of heterogeneous expression of the SOS response in clinical isolates of *Escherichia coli* on response to the fluoroquinolone, ciprofloxacin. *In silico* analysis of whole genome sequencing data showed remarkable sequence conservation of the SOS response regulators, RecA and LexA. Despite the genetic homogeneity, our results revealed a marked differential heterogeneity in SOS response activation, both at population and single-cell level, among clinical isolates of *E. coli* in the presence of subinhibitory concentrations of ciprofloxacin. Four main stages of SOS response activation were identified and correlated with cell filamentation. Interestingly, there was a correlation between clinical isolates with higher expression of the SOS response and further progression to resistance. This heterogeneity in response to DNA damage repair (mediated by the SOS response) and induced by antimicrobial agents could be a new factor with implications for bacterial evolution and survival contributing to the generation of antimicrobial resistance.

1. Introduction

Antimicrobial resistance became one of the major public health problems of the twentieth century. The continuous and often excessive use of antimicrobials to control human and animal infections has resulted in bacterial populations increasingly developing antimicrobial resistance mechanisms (Cook and Wright, 2022). Due to the high prevalence of resistance, some microorganisms are currently difficult to treat with commercially available antimicrobials. Thus, the main challenge is to discover new strategies for the use of antimicrobials (Baker et al., 2018).

Among the alternatives described in the literature, the SOS response is a promising strategy. The SOS response is an inducible stress response system that is activated when DNA is damaged, resulting in the accumulation of single-stranded DNA (ssDNA) (Maslowska et al., 2019). Induction of the SOS response can be triggered by genotoxic agents that damage DNA, such as fluoroquinolones (Rodríguez-Martínez et al., 2016). Fluoroquinolones are broad-spectrum antimicrobial agents that induce the SOS response following replication fork arrest by blocking type II topoisomerases, leading to double-strand breaks and ssDNA release (Baharoglu and Mazel, 2014). RecA binds to ssDNA, forming a nucleoprotein filament that catalyzes self-cleavage of the repressor, LexA. LexA represses genes belonging to the SOS regulon. Thus, LexA cleavage leads to the expression of more than 50 genes associated with different DNA repair mechanisms, including nucleotide excision repair (*uvr* genes), homologous recombination (*recA* gene) and translesion synthesis (*polB*, *dinB*, *umuCD* genes) (Maslowska et al., 2019). *sulA* gene expression induces inhibition of cell division, enabling errors to be fully repaired before cell division occurs (Dajkovic et al., 2008), and the *tisB* gene is involved in the formation of persister cells, which exhibit tolerance to antimicrobials (Dörr et al., 2010). It has been reported that genes involved in the SOS response are induced at different times and at

* Correspondence to: Department of Microbiology, University of Seville, Avda Sanchez Pizjuan s/n, Seville 41009, Spain.
E-mail address: sdiaz6@us.es (S. Diaz-Diaz).

https://doi.org/10.1016/j.drup.2024.101087
Received 4 December 2023; Received in revised form 22 March 2024; Accepted 18 April 2024
Available online 23 April 2024

different levels of expression (Culyba et al., 2018).

Quinolone resistance is a sequential process arising from the accumulation of chromosomal mutations in genes encoding type II topoisomerases. Although mutations in type II topoisomerases are the main mechanism of quinolone resistance, it is also mediated by other chromosomal and plasmid mechanisms (Bush et al., 2020); target protection by *qnr* genes is one of the latter. More specifically, the *qnrB* gene has a *lexA*-binding sequence in its promoter region and is involved in protecting cells from DNA damage following SOS response activation (Briales et al., 2012; Da Re et al., 2009).

Bacteria have traditionally been considered clonal populations of identical cells. However, under certain conditions, cell-to-cell fluctuations can occur in isogenic cultures (Sánchez-Romero and Casadesús, 2014; Takhaveev and Heinemann, 2018). Phenotypic heterogeneity has been described following exposure of bacteria to stress conditions, such as low nutrient levels or antimicrobial treatment (Davis and Isberg, 2016). Previous reports have shown that genes belonging to the SOS regulon are heterogeneously expressed in individual cells in response to the level of DNA damage induced by exogenous agents. The heterogeneity of the SOS response induces multiple phenotypic changes and often favors cell survival and adaptation to adverse environments (Jaramillo-Riveri et al., 2022). Most of the data come from the study of laboratory strains. The response and impact of this phenomenon on clinical isolates remain unknown.

In this context, we analyzed genetic variations of the SOS response regulators (*recA* and *lexA* genes) and genes belonging to the SOS regulon (such as the *sulA* gene) in clinical isolates of *Escherichia coli*. We found differential expression of the SOS response (*recA*, *dinB*, *tisB* and *sulA* genes) and of genes involved in fluoroquinolone resistance (*qnrB* gene) in clinical isolates exposed to sublethal concentrations of ciprofloxacin, despite high sequence conservation of the SOS response regulators. The consequences of this heterogeneity of population response in relation to its impact on antimicrobial resistance and virulence are discussed.

2. Materials and methods

2.1. Strains, growth conditions and antimicrobial agents

Twenty-six clinical isolates of *E. coli* of bacteremic or urinary origin were included in this study (Machuca et al., 2021). The reference strain was *E. coli* MG1655. The *recA* gene was disrupted following a modified version of the method described by Datsenko and Wanner (Datsenko and Wanner, 2000; Machuca et al., 2021). Green fluorescent protein (GFP) expression from the pMS-PrecA::gfp, pMS-PdinB::gfp, pMS-PtisB::gfp, pMS-PsulA::gfp, pMS-PqnrB::gfp vectors were used to display *recA*, *dinB*, *tisB*, *sulA* and *qnrB* promoter activity (SOS induction) (Zaslaver et al., 2006). The pCA24N-recA plasmid was also electroporated into MG1655 Δ*recA* pMS-PrecA::gfp for genotype and phenotype complementation.

Strains were grown at 37 ºC. Ciprofloxacin was used for the various assays (Sigma-Aldrich, Madrid, Spain). Kanamycin (50 mg/L; Sigma-Aldrich, Madrid, Spain) was used for plasmid maintenance.

2.2. Characterization of recA and lexA genes in complete genomes available

All complete genome assemblies of *E. coli* available in the RefSeq database in October 2021 were downloaded, creating a genomic dataset of 2053 isolates. Sequences of *recA* and *lexA* genes in the genomes were identified by homology search using blastn v2.10.1+ (Camacho et al., 2009), translated into amino acids and aligned and trimmed with mafft-linsi v7.475 and trimAl v1.4.rev15 (option –gappyout), respectively (Capella-Gutiérrez et al., 2009; Katoh et al., 2018). Finally, all sequence alignments were visualized in SeaView (Gouy et al., 2021).

2.3. Characterization of promoter sequences in complete genomes available

A 250 bp nucleotide region upstream of the *recA* and *lexA* genes was extracted from the complete genome dataset. Unique promoter sequences were obtained using Ecocyc (Keseler et al., 2021) to characterize their internal structure. Finally, the WebLogo v.2.8.2 tool was used to represent the base composition of unique promoter sequences (Crooks et al., 2004).

2.4. Whole-genome sequencing of a clinical isolate collection

The twenty-six clinical isolates were subjected to whole-genome sequencing on the Miseq platform (Illumina, San Diego, CA). Libraries were prepared with the Nextera XT DNA library preparation kit and loaded onto a V3 600-cycle reagent cartridge for sequencing. Illumina sequences were assembled *de novo* using the CLC Genomics Workbench (Qiagen, Netherlands). The genomes were annotated with Rapid Annotation using Subsystem Technology (RAST) (Aziz et al., 2008). *recA*, *lexA,* and *sulA* gene and amino acid sequences were compared with the reference genome of *E. coli* K-12 substr. MG1655 (Keseler et al., 2021), using the NCBI BLAST online application.

2.5. Minimum Inhibitory Concentration (MIC) determination and fluorescence detection by disk diffusion

The Kirby-Bauer disk diffusion susceptibility test was used (Bauer et al., 1966). Briefly, bacteria grown overnight on Mueller–Hinton media were diluted to a 0.5 McFarland standard (ca. 10^8 cells/mL). The cell suspensions were spread evenly over Mueller–Hinton agar plates using sterile cotton swabs, and antimicrobial disks (Oxoid) or gradient strips (Liofilchem) were applied. Plates were incubated for 24 h at 37 °C. Ciprofloxacin MICs obtained using the gradient strip technique were determined in triplicate for each bacterial strain. Fluorescence halos obtained using ciprofloxacin disks were visualized with Safe Imager™ 2.0 (Invitrogen, Spain).

2.6. Determination of gene promoter activity by growth curves

Bacterial growth curves were performed to highlight differences in *recA* gene expression between different clinical isolates of *E. coli*, including *recA*-deficient clinical isolates. Transparent 96-well flat-bottom plates containing 200 µL of sublethal concentrations of ciprofloxacin (1/4xMIC for each clinical isolate) in M9 minimal medium supplemented with 20% glucose were prepared to induce a bacterial stress response, as previously described, using the Infinite 200 PRO plate reader (Tecan, Madrid, Spain). The initial inoculum was 10^6 cells/mL. Fluorescence was measured (fluorescence excitation at 485±20 nm and emission at 535±25 nm) and normalized to optical density, measured at 595±10 nm during 24 hours. The means of at least three biological replicates were represented.

2.7. Determination of gene promoter activity by flow cytometry

For strain preparation, a 1:100 dilution of a 0.5 McFarland was prepared in M9 minimal medium (10^6 cells/mL). Cells were exposed to 1/16x-1xMIC of ciprofloxacin for each strain for 3 and 6 hours at 37 ºC. Next, 10 mL of cell culture was centrifuged for 15 mins at 4600 rpm and washed twice in 2 mL of saline solution 0.9%. Flow cytometry acquisition was performed at a low flow rate (~30 events/s) using a BD FACS Canto II BC500 (Beckman Coulter) cytometer, measuring GFP fluorescence with the blue laser (excitation at 488 nm, detection at 530 ±30 nm). At least 50,000 cells per sample were collected using BD FACSDiva software and analyzed with FlowJo™ v10.8 Software (BD Life Sciences).

2.8. Analysis of cell elongation by fluorescence microscopy

For strain preparation, a 1:100 dilution of a 0.5 McFarland was prepared in M9 minimal medium (10^6 cells/mL). Cells were then exposed to concentrations of 1/4xMIC of ciprofloxacin for each strain for 6 hours at 37 ºC. 1 mL aliquots were centrifuged for 3 min at 15,000 rpm, resuspended in 1 mL of 10^{-2} M of $MgSO_4$ and incubated for 10 min at 4 °C.

For optimal visualization by fluorescence microscopy and to ensure immobilization of cells for better image acquisition, an agarose pad was placed on the microscope slides. The matrix gel was prepared by dissolving 0.15 g of agarose (Sigma-Aldrich) in 50 mL of 10^{-2} M of $MgSO_4$. An adhesive chamber slide system (Thermo Fisher Scientific) was placed over the slides, 250 μL of matrix was poured and allowed to dry at 4 °C for 1 hour. Small drops of approximately 1.5 μL of the prepared cells were placed on the slides and allowed to dry before covering with coverslips.

Conventional wide-field fluorescence microscopy imaging was carried out on a Carl Zeiss™ Axio Vert. A1 FL-LED inverted microscope, equipped with an Axiocam503c camera. Fluorescence microscope images taken at 40x magnification were acquired using ZEN 2 software (blue edition, version 2.0). Microscopy images were analyzed using the free MicrobeJ plugin (Ducret et al., 2016). For automated detection of possible cells with longer filaments, the following parameters were used: Length: 35–150,000 px (1.6–6750 μm); area: 100–250,000 px^2 (4.5–11, 250 μm^2); width: 0-max; circularity: 0-max; curvature: 0–0.8 px; sinuosity: 0-max; angularity: 0–0.8 rad; solidity: 0-max. When necessary, cell contours were corrected using the manual editing interface of the MicrobeJ plugin. In accordance with ZEN 2 software scaling, all pixel measurements were converted to μm using the ratio provided by the developers: 0.045 μm/px. For each strain and condition, a minimum of 100 and a maximum of 1500 cells were analyzed.

2.9. Agar gradient plate experiments

A key aspect of bacterial survival is the ability to evolve while migrating through spatially varying environmental challenges (Baym et al., 2016; Recacha et al., 2019). Gradient plate assays (120.5 mm) were used to evaluate microbial evolution as a function of the SOS response. A maximum ciprofloxacin concentration of 4xMIC (relative to the wild-type SOS response) and BM2 swarm medium were used (Overhage et al., 2008). Each plate was first tilted at an angle of 5 degrees from the horizontal and a first layer of molten agar containing selective agents was added (30 mL). After the initial layer had hardened, the plate was laid flat and a second layer of molten agar without selective agents was poured onto the plates (30 mL). For strain preparation, a 1:100 dilution of a 0.5 McFarland was prepared (10^6 cells/mL). The plates were inoculated with 5 μl of the 1:100 dilution and incubated for a maximum of 240 h. Finally, images were taken and the main evolutionary lineages were recorded manually.

2.10. Statistical analysis

All statistical analyses were performed using Graphpad Prism 6 software (https://www.graphpad.com). The Student's t-test was used to compare two groups. Linear regression analysis was also performed. Differences were considered significant when p values were <0.05.

3. Results

3.1. Conserved genetic sequences of the main regulators of the SOS response: LexA and RecA

After identification and characterization of RecA and LexA amino acid sequences from a dataset of 2053 *E. coli* sequences, unique amino acid variants containing at least one change compared to wild-type *E. coli* MG1655 were identified. With respect to the RecA sequences, the wild-type variant was represented by 1989 sequences. Another 14 variants were less frequent, each represented by 19 sequences or fewer (Figure S1). LexA sequences showed fewer variants. The wild-type variant was represented by 2035 sequences. Another 8 variants were each represented by 7 sequences or fewer (Figure S2). The *recA* and *lexA* promoter regions were also analyzed. With respect to the *lexA* promoter region, no differences were observed in the regulatory box sequences at −10 and −35, although changes of one and two nucleotides, respectively, were observed in the two *lexA* regulatory boxes (Figure S3A). In the *recA* promoter region, there were no nucleotide changes in the regulatory box sequences at −10, but one change was observed in the −35 regulatory box, and three in the *lexA* regulatory box (Figure S3B).

To evaluate genetic variations in SOS response regulators in the collection of twenty-six *E. coli* clinical isolates, the nucleotide and amino acid sequences of *lexA* and *recA*, as well as their promoter regions, were analyzed and compared with those of wild-type *E. coli* MG1655. For the open reading frame (ORF) gene sequences, some differences in nucleotide sequences were observed, although they never translated into amino acid differences. Unlike the database sequences, no variations were observed in the promoter regions of the two genes (data available at BioProject PRJNA1015411). These data confirm the high degree of conservation of the genetic context of the main SOS response regulators in the database genomes that were available and in our study collection.

In addition, analysis of the promoter region and amino acid sequence of SulA (part of the SOS regulon and important for filamentation and virulence) showed that the wild-type MG1655 amino acid sequence was identical to that of clinical isolates FI11, FI7, FI8, FI9, FI13, FI12, FI13, FI18 and FI19. Five other variants were identified: v1, including FI1; v2, including FI5 and FI6; v3, including FI10; v4, including FI14 and FI16; and v5, including FI4, FI15, FI17 and FI20-FI27 (Table S1). With respect to the promoter region, no differences were observed in the regulatory boxes at −10 and −35 or the two RcdA regulatory boxes (stress response transcriptional regulators) located within the *sulA* gene sequence, although four nucleotide differences were observed in the *lexA* regulatory box (Figure S4).

3.2. Heterogeneity of recA gene expression at whole population level

The MIC values of ciprofloxacin for clinical isolates and the wild-type MG1655 strain were as follows: 0.015 mg/L for MG1655 and FI1; 0.06 mg/L for FI26; 0.125 mg/L for FI21; 0.25 mg/L for FI5, FI7, FI8, FI9, FI10 and FI22; 0.5 mg/L for FI6, FI11, FI13, FI14, FI15, FI16 and FI17; 2 mg/L for FI20; 16 mg/L for FI19; and 32 mg/L for FI23, FI25 and FI27. Hence, this collection provides a representative cross-section of susceptible, low-level resistant, and quinolone-resistant phenotypes (Machuca et al., 2021). There was a 4–16-fold reduction in the ciprofloxacin MIC for isolates with deletion of the *recA* gene compared with their corresponding wild-type strains, while complementation of *recA* with the pCA24N-recA plasmid of a *recA*-deficient MG1655 strain restored the wild-type MIC (Table S2).

Despite the genetic similarity of *recA* sequences among the clinical isolates, clear differences in the expression of the SOS response were observed. Different fluorescence intensities were observed among the clinical isolates under ciprofloxacin pressure by disk diffusion (Fig. 1, grouped according to the criteria set out in Fig. 2). Mild or no fluorescence was observed in *recA*-deficient strains (Fig. 1). Complementation of *recA* with a pCA24N-recA plasmid in a *recA*-deficient MG1655 strain restored *recA* gene expression (Fig. 1A). The expression of other genes involved in the SOS response (*dinB*, *tisB* and *sulA*), as well as a plasmid-mediated quinolone resistance gene (*qnrB*), was also evaluated (Figure S5). A differential level of expression was observed for all genes evaluated in clinical isolates FI22 and FI14, with higher expression in the latter. As expected, fluorescence was not observed in *recA*-deficient clinical isolates, confirming suppression of the SOS response (Figure S5).

recA gene expression was also evaluated over the course of the

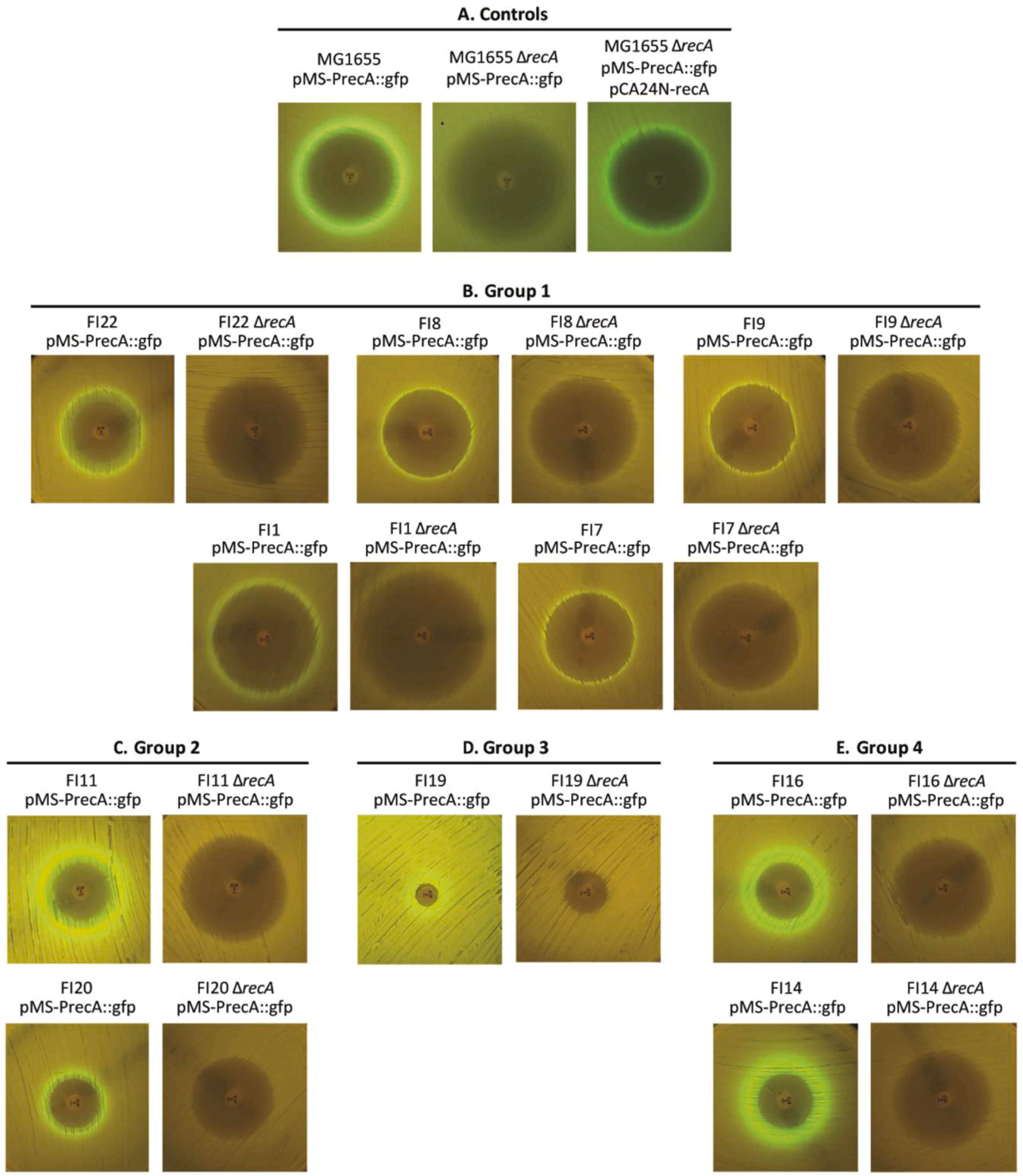

Fig. 1. Monitoring of the SOS response in wild-type *E. coli* MG1655 (A), *E. coli* clinical isolates (B-E) and their isogenic pairs with inactivation of the *recA* gene, by disk diffusion using ciprofloxacin (5 μg) and read at 24 hours. Green fluorescent protein (GFP) expression from the pMS-PrecA::gfp vector was used to display *recA* promoter activity (SOS induction) after addition of ciprofloxacin.

growth curves using 1/4xMIC of ciprofloxacin for each strain (Fig. 2A and S6). At 6 hours, four groups of clinical isolates were established according to fluorescence level ($p<0.05$). The first group showed the lowest fluorescence intensity, which ranged from 158 to 286 units, and included the FI22, FI8, FI9, FI1, FI17, FI7, FI21, FI26 and *recA*-deficient clinical isolates. The second group ranged from 448 to 726 units, and included clinical isolates FI13, FI27, FI11, FI20 and FI15 and wild-type MG1655, and *recA*-deficient MG1655 complemented with the pCA24N-recA plasmid. The third group ranged from 787 to 918 units and included clinical isolates FI19, FI6, FI5 and FI23. Finally, the fourth

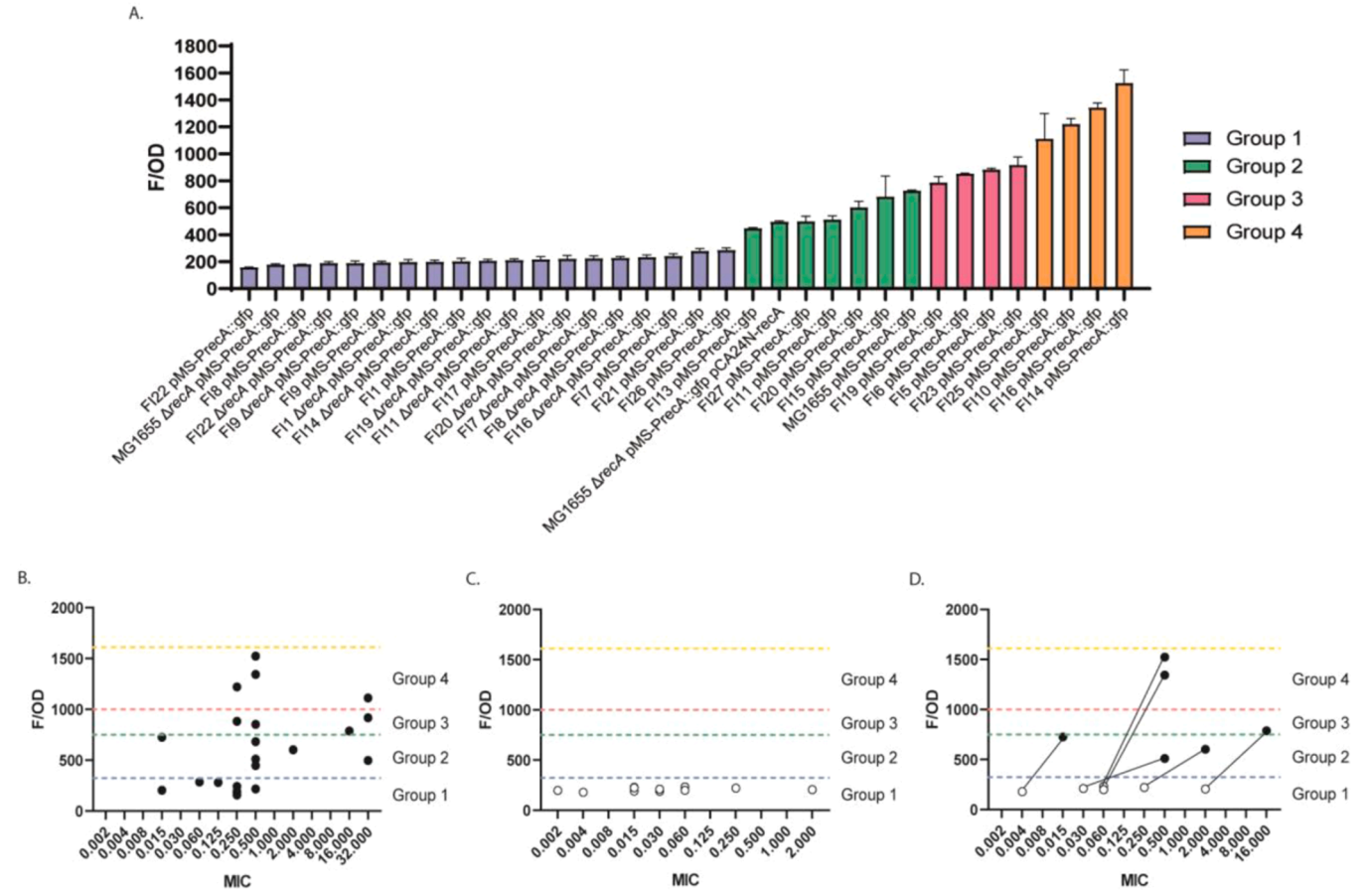

Fig. 2. Clinical isolates of *E. coli* exhibit differential *recA* gene expression (SOS response). Fluorescence normalized to optical density (OD595nm) was measured after 6 hours of treatment with 1/4xMIC of ciprofloxacin for each strain. Four groups were established according to the level of fluorescence exhibited: Group 1 is shown in blue, Group 2 in green, Group 3 in pink, and Group 4 in orange. The means of at least three independent measurements are plotted. MG1655, MG1655 Δ*recA* and MG1655 Δ*recA* pCA24N-recA were used as control strains (A). Association between MIC values and *recA* gene expression measured by growth curves of *E. coli* clinical isolates (B) and *recA*-deficient clinical isolates (C). Reductions in the levels of susceptibility and *recA* gene expression in *recA*-deficient clinical isolates compared with their respective wild-type clinical isolates are represented by black lines (D).

group showed the highest fluorescence intensity, ranged from 1113 to 1525 units, and included clinical isolates FI25, FI10, FI16 and FI14 (Fig. 2A). The differences in expression between the four groups can also be clearly observed over 24 h (Figure S6). Interestingly, clinical isolates with the same MIC value showed differential levels of *recA* gene expression. Thus, clinical isolates which had an MIC value of 0.25 mg/L belonged to group 1 (FI7, FI8, FI9 and FI22), group 3 (FI5) and group 4 (FI10); clinical isolates with MIC values of 0.5 mg/L belonged to group 1 (FI17), group 2 (FI11 and FI13), group 3 (FI15 and FI6) and group 4 (FI14 and FI16); and clinical isolates whose MIC value was 32 mg/L belonged to group 2 (FI27), group 3 (FI23) and group 4 (FI25) (Fig. 2B). Linear regression analysis showed no correlation between MIC value and *recA* gene expression level (R^2=0.06). As expected, *recA*-deficient clinical isolates not only showed a decreased level of *recA* gene expression (Fig. 2C), but also a reduced level of susceptibility (Fig. 2D).

3.3. Heterogeneity of recA gene expression at single-cell level

The heterogeneity of *recA* gene expression among clinical isolates was further evaluated by flow cytometry at the single-cell level. Based on the level of induction of untreated clinical isolates, a FITC value of $10^{3.5}$ was established as the cut-off point (differential threshold to define SOS response induction) dividing bacterial cells into two populations (P1 and P2). Significant differences in the number of cells in P2 were observed between clinical isolates ($p<0.05$) (Fig. 3 and S7, Table S3). Clinical isolates belonging to group 1 (FI22, FI8, FI9, FI1 and FI7) showed less than 30% of cells in P2; clinical isolate FI20 (group 2) showed 33.5%; clinical isolate FI19 (group 3) showed 70%; and clinical isolates belonging to group 4 showed 90.2% (FI16) and 93.4% (FI14) in P2. Although clinical isolate FI11 was classified as group 2 after growth curve analysis at population level, it resembled group 4 at single-cell level by flow cytometry, showing 88.3% of cells in P2. As expected, almost 100% of cells in *recA*-deficient clinical isolates were located in P1. Complementation of *recA* with the pCA24N-recA plasmid in a *recA*-deficient MG1655 strain restored *recA* gene expression, with 62.8% of cells in P2 (Fig. 3B, Table S3). Untreated clinical isolates showed 100% of cells in P1 (Fig. 3A, Table S3). In other clinical isolates analyzed, differential levels of *recA* gene expression were confirmed (Figure S7, Table S3). In general, single-cell level data showed a high degree of concordance with the whole population analysis, as well as variability in heterogeneity in expression of the SOS response, in which it was even possible to observe different subpopulations in terms of response intensity (FI11, FI16 and FI14 clinical isolates) (Figure S8). Interestingly, differences in *recA* gene expression between groups can be observed at shorter times (3 hours) and at different concentrations [1/16xMIC, 1/8xMIC, 1/4xMIC, 1/2xMIC and 1xMIC (Figures S9 and S10)]. Moreover, these differences are observed even when clinical isolates are treated with UV light (data not shown).

Analysis of the expression of *dinB*, *tisB*, *sulA* and *qnrB* genes, evaluated specifically in clinical isolates FI14 and FI22 and their respective *recA*-deficient isogenic pairs, also showed clear and significant differences in expression between FI14 (more than 43.2% of cells in P2) and

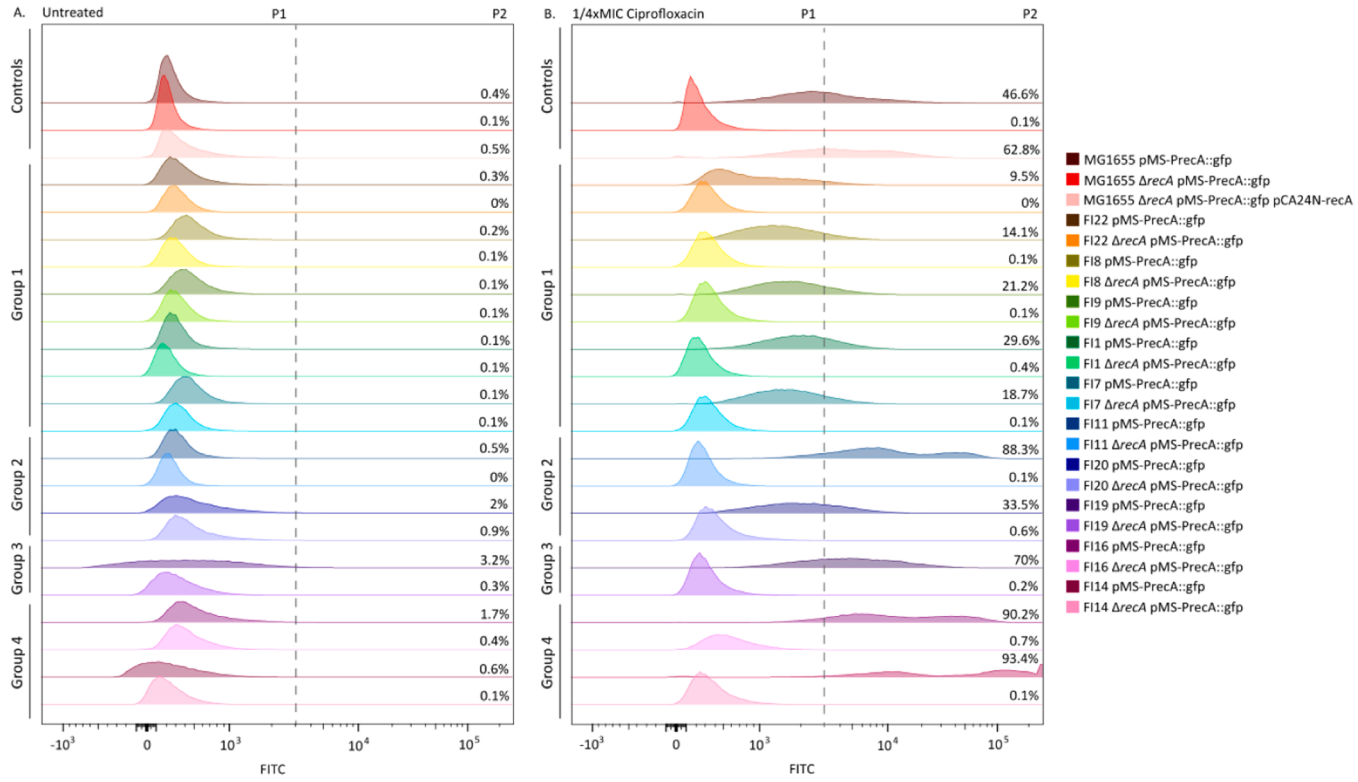

Fig. 3. Flow cytometry evaluation of heterogeneous expression of the *recA* gene at single-cell level in clinical isolates of *E. coli* and their isogenic pairs with inactivated *recA* gene after 6 hours without treatment (A), and with treatment using a ciprofloxcin concentration of 1/4xMIC for each strain (B). Bacterial cells divided into two populations (P1 and P2) using a FITC value of $10^{3.5}$ as the cut-off point (vertical dashed line) are also represented. Percentages of bacterial cells in P2 are shown on the right. MG1655, MG1655 Δ*recA* and MG1655 Δ*recA* pCA24N-recA were used as control strains.

FI22 (less than 6.7% of cells in P2) ($p<0.05$), which also confirms differential expression in the effectors of the SOS response. As expected, in *recA*-deficient clinical isolates, 100% of cells belonged to P1 (Table S3).

3.4. Heterogeneity of cell filamentation correlates with heterogeneity of the SOS response

As part of the SOS response, *sulA* gene expression induces inhibition of cell division. Accordingly, cell filamentation was evaluated in *E. coli* clinical isolates, as well as in *recA*-deficient clinical isolates (Table S4). The extent of cell filamentation was observed to vary among clinical isolates, being lower in clinical isolates of group 1 and higher in those of group 4 ($p<0.05$) (Fig. 4, Table S4). More specifically, under ciprofloxacin pressure, clinical isolates belonging to group 1 showed mean length of 2.5–4.6 μm and mean area of 34.6–53.1 μm^2; those from group 2 showed mean length of 2.8–5.7 μm and mean area of 31.5–69.9 μm^2, except for clinical isolate FI15, which showed higher values (mean length 9.3 μm and mean area 110.4 μm^2); group 3 showed mean length of 4.2–5.9 μm and mean area of 49–74 μm^2; and group 4, a mean length of 4–8.9 μm and mean area of 48.3–124.1 μm^2. The results for *recA*-deficient clinical isolates were similar to those for group 1 (mean length 2–3 μm, mean area 27–30 μm^2). More specifically, average cell lengths and areas peaked at 11.4 μm and 158 μm^2 (group 1 strains), 25.8 μm and 324.7 μm^2 (group 2); 23.5 μm and 328.4 μm^2 group 3), 46.3 μm and 597.5 μm^2 (group 4), and 8.1 μm and 98.9 μm^2 (*recA*-deficient clinical isolates). As expected, the lengths and areas of all untreated clinical isolates did not change, with values around 2–3 μm and 20–37 μm^2, respectively (Table S4).

In general, a correlation was established, both at the whole population and single-cell level, between SOS response activity, assessed indirectly by measuring fluorescence emissions after *recA* gene induction, and cell filamentation, measured directly on images acquired by fluorescence microscopy (Fig. 4A-B). High induction of the SOS response correlated with a high level of cell filamentation. Nevertheless, some exceptions were observed, such as clinical isolate FI15, which showed high levels of cell filamentation despite intermediate expression of the SOS response, and clinical isolates FI10 and FI25 which showed low levels of cell filamentation despite high expression of the SOS response (Fig. 4A-B). Fig. 4C-F shows representative images of different levels of cell filamentation observed according to the level of expression of the SOS response.

3.5. Spatiotemporal microbial evolution in E. coli clinical isolates varies according to their expression of the recA gene

The ability to evolve toward adaptation to ciprofloxacin was evaluated in strains showing low (FI22 clinical isolate) and high (FI14 clinical isolate) expression of the SOS response (Fig. 5). The progression to higher levels of ciprofloxacin resistance differed between the two clinical isolates, being higher in the case of FI14 which showed higher *recA* gene expression (Figs. 5A and C). The main evolutionary lineages were recorded, however, in the case of clinical isolate FI14 multiple lineages were not indicated due to their reduced size. Despite this, interestingly, clinical isolate FI14 showed 41 microbial lineages (Fig. 5C), in contrast to clinical isolate FI22 that showed 9 lineages (Fig. 5A). Surprisingly, the emergence of multiple evolutionary lineages with different fluorescence intensities and displaying various levels of *recA* gene expression was observed in clinical isolate FI14 (Fig. 5C). As expected, there was a marked delay in the spatiotemporal evolution of ciprofloxacin resistance in the two *recA*-deficient clinical isolates of *E. coli* with *recA*-deficient clinical isolate FI22 showing 1 lineage (the original one) (Fig. 5B) and *recA*-deficient clinical isolate FI14 showing 7 lineages (Fig. 5D). Other clinical isolates from group 1 (FI1 and FI7 clinical isolates) and group 4 (FI10 and FI25 clinical isolates) were also evaluated, showing a greater

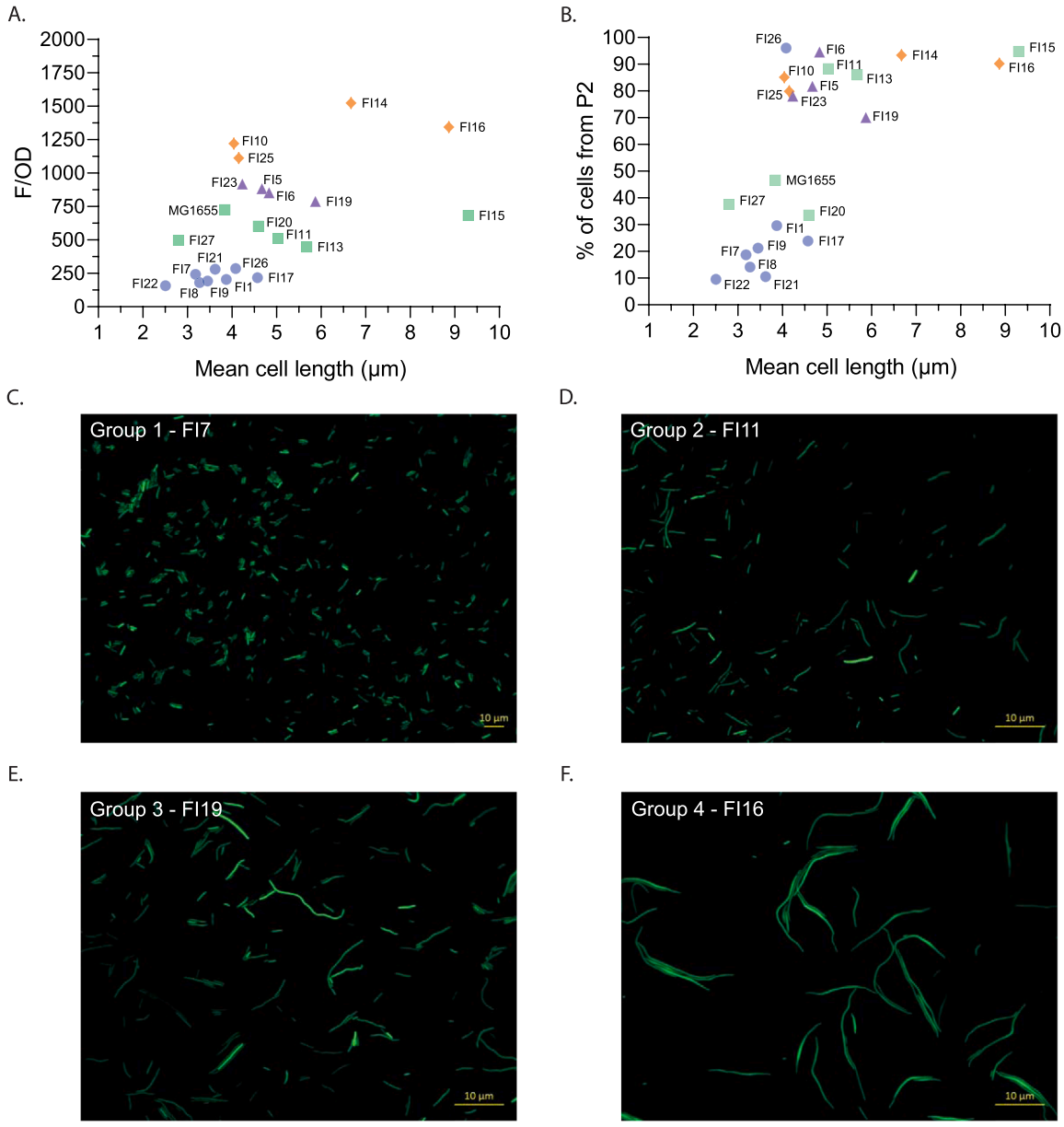

Fig. 4. Correlation between cell elongation and *recA* gene expression. Mean cell length (μm) versus fluorescence normalized to optical density (F/OD). (A). Mean cell length (μm) versus the percentage of cells of each isolate belonging to population 2 (P2), using the flow cytometry cut-off point of $10^{3.5}$ (B). Evaluation of cell elongation by fluorescence microscopy at 40x magnification in *E. coli* clinical isolates FI7 from group 1 (C), FI11 from group 2 (D), FI19 from group 3 (E), and FI16 from group 4 (F) after 6 hours of exposure to 1/4xMIC of ciprofloxacin. MG1655 was used as the reference strain. Blue dots: group 1; green squares: group 2; violet triangles: group 3; orange diamonds: group 4.

progression towards ciprofloxacin resistance in the case of clinical isolates with higher expression of the *recA* gene (Figure S11).

4. Discussion

Since the emergence of antimicrobial resistance, efforts have focused on discovering the mechanisms that enable bacteria to withstand antimicrobial stress in order to identify potential targets for use as novel antimicrobial strategies. Decades of genetic profiling of antimicrobial-resistant isolates have shown that multiple genetic alterations acting together shape the final resistance phenotype (Hughes and Andersson, 2017).

Interestingly, while a heterogeneous response to antimicrobials has frequently been observed due to genetic diversity, phenotypic heterogeneity can often be observed in a genetically identical population (Davis and Isberg, 2016). Heterogeneity within a bacterial population can be a great advantage since, under certain potentially lethal conditions, some cells are able to survive and adapt to new environments (Davis, 2020). Sánchez-Romero and Casadesús studied the expression of outer membrane porins in kanamycin-resistant *S. enterica* cultures and identified heterogeneous expression leading to different levels of kanamycin resistance (Sánchez-Romero and Casadesús, 2014). This is consistent with our study observations of heterogeneous expression of the SOS response at both population and single-cell levels in the analyzed *E. coli* clinical isolates in spite of the sequence similarity of the SOS response regulators, RecA and LexA, as well as their promoter regions (Figs. 1, 2, 3 and S7, Table S3). Furthermore, the analysis of database sequences confirmed the high conservation of the SOS response regulators in clinical isolates of *E. coli* (Figure S1, S2 and S3). In this study, four main potential activation levels of SOS response were

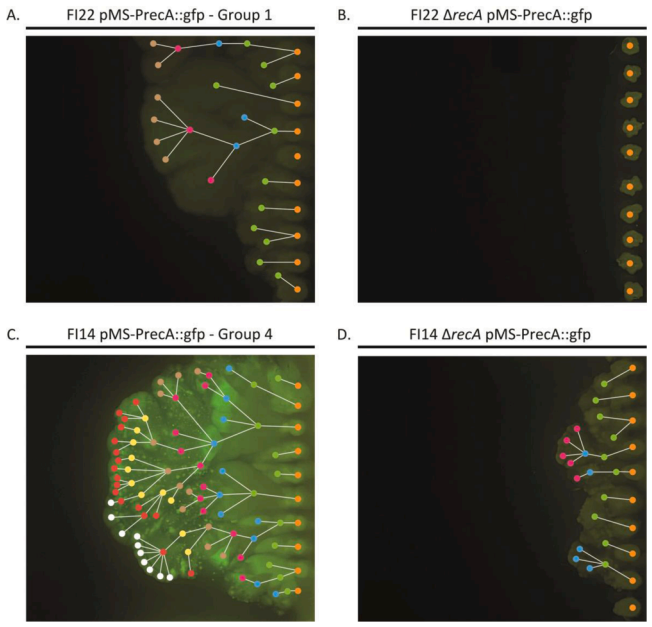

Fig. 5. Agar gradient plate experiments to examine spatiotemporal microbial evolution. Swimming motility of *E. coli* FI22 (clinical isolate from group 1) (A) and FI14 (clinical isolate from group 4) (C) and their isogenic pairs with inactivation of the *recA* gene (B,D) at 4xMIC of ciprofloxacin relative to the wild-type after 240 hours of microbial evolution. *recA* gene expression, associated with activation of the SOS response, was also evaluated using the pMS-PrecA::gfp vector. Evolutionary lineages are represented by lines and dots.

established: no induction (group 1, including *recA*-deficient strains), mild induction (group 2, including wild-type MG1655), high induction (group 3) and very high induction (group 4). Most of these clinical isolates showed little SOS response activation and were included, together with the *recA*-deficient strains, in group 1. However, the fact that wild-type *E. coli* MG1655 showed a higher expression of the SOS response (group 2) indicates that, with remarkable frequency, the sub-inhibitory concentrations of ciprofloxacin used did not induce a significant SOS response in *E. coli* clinical isolates (Group 1 for Figs. 2, 3 and S7). Interestingly, heterogeneous expression of the SOS response was independent of the level of susceptibility (Fig. 2B). Another interesting observation is that clinical isolates with low-level quinolone resistance showed higher variability in SOS response (Fig. 2B), which could be an advantage for this phenotype. In view of the above, both susceptible and resistant phenotypes could benefit from the SOS response in terms of their stress responses and ability to evolve. Further studies are needed to determine if there are other mechanisms that explain the observed differences in the expression of the SOS response.

Previous studies have shown that genes involved in the SOS response are heterogeneously expressed in individual cells in response to naturally occurring DNA damage or damage caused by exogenous agents such as antimicrobials (Jaramillo-Riveri et al., 2022; Jones and Uphoff, 2021). Heterogeneous induction of the SOS response could be due to different levels of damage to the genetic material, variability in the repair process, or differential activation of the SOS response genes (Vincent and Uphoff, 2020). This line of results is consistent with the data in this study on the heterogeneity of SOS response expression in clinical isolates of *E. coli*. Furthermore, our study evaluated genes involved in DNA repair (*dinB* gene), cell division inhibition (*sulA* gene), persister cell formation (*tisB* gene) and genes associated with fluoroquinolone resistance regulated by a *lexA* box (*qnrB* gene) (Figure S5, Table S3), and confirmed differential expression among clinical isolates, despite the fact that these genes are induced at different times and with different levels of expression (Culyba et al., 2018). Such variability could therefore have consequences in terms of the evolution, virulence, persistence or acquisition of antimicrobial resistance.

The SOS response is a very strong but transient response to genotoxic stress, during which bacteria are able, not only to repair their DNA, but also to reorganize and mutate their genome by expressing low-fidelity polymerases (Crane et al., 2021). High mutation frequencies are more likely to confer deleterious than beneficial traits, demonstrating that induction of the SOS response requires fine-tuned control to achieve mutability levels that are both adequate and favorable (Blázquez et al., 2018). Heterogeneity of the SOS response, given its role in DNA repair, is capable of inducing a variety of phenotypic changes, some of which favor cell survival, evolution and general adaptation to harsh environments (Jaramillo-Riveri et al., 2022; Mérida-floriano et al., 2021). In terms of the ability to evolve to ciprofloxacin resistance, evaluated in two strains, one with no induction (clinical isolate FI22) and one with very high induction (clinical isolate FI14) of the *recA* gene (SOS response), progression to resistance was greater in the clinical isolate with higher expression of the SOS response (Fig. 5). Indeed, the involvement of the SOS response in the emergence of antibiotic resistance was demonstrated by inactivating the SOS response in repair-deficient hypermutator strains, which showed reduced rates of resistance development (Cirz and Romesberg, 2006; Recacha et al., 2017).

Bos et al., among others, established a correlation between an antibiotic-induced SOS response and cell filamentation, noting that most cells with very high levels of SOS expression had delayed or arrested division, consistent with induction of the SOS-dependent cell division inhibitor SulA (Bos et al., 2015). Concerning cell division, their time-lapse data suggested that two distinct subpopulations could be observed: one dividing normally, with relatively low or intermediate SOS expression levels, and a second one dividing very slowly, with high SOS expression levels (Bos et al., 2015). Following on from this, in our study, an overall positive correlation was found between SOS response expression and cell filamentation in clinical isolates of *E. coli*, whereby those with increased expression of the SOS response showed increased cell filamentation (Fig. 4, Table S4). The increased expression of the SOS response and, therefore, increased filamentation could have an impact in mutagenesis as has been described in other studies (Bos et al., 2015; Pribis et al., 2019). Even so, the analysis of the promoter region and amino acid sequence of SulA revealed no association with the observed differences in cell filamentation in *E. coli* clinical isolates (Figure S4, Table S1).

Overall, beyond the high conservation of sequences of the SOS response regulators (RecA and LexA), we highlight a heterogeneous SOS response expression, among clinical isolates of *E. coli* in response to antimicrobials like ciprofloxacin. Our findings raise the possibility that a differential DNA damage repair response may contribute to the ways in which *E. coli* clinical isolates interact with antimicrobials. Further in-depth studies are needed to identify the key drivers of a differential SOS response in *E. coli* clinical isolates.

Funding

This work was supported by the Plan Nacional de I+D+i 2013-2016 and the Instituto de Salud Carlos III (project PI20/00239). Sara Diaz-Diaz is supported by a PFIS fellowship from the Instituto de Salud Carlos III (FI18/00086), co-funded by ESF "Investing in your future"; Esther Recacha is supported by a Juan Rodés fellowship from the Instituto de Salud Carlos III (JR21/00030), co-funded by ESF "Investing in your future"; Marina R. Pulido is supported by a VIPPI-US fellowship from the University of Seville; María Romero-Muñoz is supported by the Fondo Social Europeo (Programa Iniciativa de Empleo Juvenil); Marina Murillo-Torres is supported by a predoctoral fellowship from the Junta de Andalucía (PREDOC_00923).

CRediT authorship contribution statement

Sara Díaz Díaz: Writing – review & editing, Writing – original draft, Visualization, Validation, Methodology, Investigation, Formal analysis, Conceptualization. **Esther Recacha:** Writing – review & editing, Conceptualization. **Marina R. Pulido:** Writing – review & editing, Methodology, Investigation, Conceptualization. **Andrea Garcia Montaner:** Writing – review & editing, Formal analysis. **Roberta Vanni:** Writing – review & editing, Methodology, Investigation, Formal analysis. **Fernando Docobo Pérez:** Writing – review & editing, Conceptualization. **Álvaro Pascual:** Writing – review & editing, Funding acquisition. **María Romero Muñoz:** Writing – review & editing, Methodology, Investigation. **Marina Murillo Torres:** Writing – review & editing, Methodology, Investigation. **José Manuel Rodríguez Martínez:** Writing – review & editing, Writing – original draft, Supervision, Investigation, Funding acquisition, Formal analysis, Conceptualization.

Declaration of Competing Interest

On behalf of all authors, I declare that we have no commercial interests related to the submitted manuscript.

Acknowledgements

The authors would like to thank Dr. Ivan Matic for the fluorescence microscopy methodology and analysis of microscopy images used in this study, as well as his contributions to the discussion of this work.

Transparency declarations

None to declare.

Sequence information

Sequencing data are provided in the NCBI (SRA) database under the study accession code PRJNA1015411.

Appendix A. Supporting information

Supplementary data associated with this article can be found in the online version at doi:10.1016/j.drup.2024.101087.

References

Aziz, R.K., Bartels, D., Best, A., DeJongh, M., Disz, T., Edwards, R.A., Formsma, K., Gerdes, S., Glass, E.M., Kubal, M., Meyer, F., Olsen, G.J., Olson, R., Osterman, A.L., Overbeek, R.A., McNeil, L.K., Paarmann, D., Paczian, T., Parrello, B., Pusch, G.D., Reich, C., Stevens, R., Vassieva, O., Vonstein, V., Wilke, A., Zagnitko, O., 2008. The RAST Server: rapid annotations using subsystems technology. BMC Genom. 9 https://doi.org/10.1186/1471-2164-9-75.

Baharoglu, Z., Mazel, D., 2014. SOS, the formidable strategy of bacteria against aggressions. FEMS Microbiol. Rev. https://doi.org/10.1111/1574-6976.12077.

Baker, S.J., Payne, D.J., Rappuoli, R., De Gregorio, E., 2018. Technologies to address antimicrobial resistance. Proc. Natl. Acad. Sci. U. S. A. https://doi.org/10.1073/pnas.1717160115.

Bauer, A.W., Kirby, W.M., Sherris, J.C., Turck, M., 1966. Antibiotic susceptibility testing by a standardized single disk method. Tech. Bull. Regist. Med. Technol. 36, 49–52.

Baym, M., Lieberman, T.D., Kelsic, E.D., Chait, R., Gross, R., Yelin, I., Kishony, R., 2016. Spatiotemporal microbial evolution on antibiotic landscapes. Sci. (80-.) 353, 1147–1151. https://doi.org/10.1126/science.aag0822.

Blázquez, J., Rodríguez-Beltrán, J., Matic, I., 2018. Antibiotic-induced genetic variation: how it arises and how it can be prevented. Annu. Rev. Microbiol. https://doi.org/10.1146/annurev-micro-090817-062139.

Bos, J., Zhang, Q., Vyawahare, S., Rogers, E., Rosenberg, S.M., Austin, R.H., 2015. Emergence of antibiotic resistance from multinucleated bacterial filaments. Proc. Natl. Acad. Sci. 112, 178–183. https://doi.org/10.1073/pnas.1420702111.

Briales, A., Rodriguez-Martinez, J.M., Velasco, C., Machuca, J., Díaz de alba, P., Blazquez, J., Pascual, A., 2012. Exposure to diverse antimicrobials induces the expression of qnrB1, qnrd and smaqnr genes by SOS-dependent regulation. J. Antimicrob. Chemother. 67, 2854–2859. https://doi.org/10.1093/jac/dks326.

Bush, N.G., Diez-Santos, I., Abbott, L.R., Maxwell, A., 2020. Quinolones: mechanism, lethality and their contributions to antibiotic resistance. Molecules. https://doi.org/10.3390/molecules25235662.

Camacho, C., Coulouris, G., Avagyan, V., Ma, N., Papadopoulos, J., Bealer, K., Madden, T.L., 2009. BLAST+: architecture and applications. BMC Bioinforma. 10 https://doi.org/10.1186/1471-2105-10-421.

Capella-Gutiérrez, S., Silla-Martínez, J.M., Gabaldón, T., 2009. trimAl: a tool for automated alignment trimming in large-scale phylogenetic analyses. Bioinformatics 25, 1972–1973. https://doi.org/10.1093/bioinformatics/btp348.

Cirz, R.T., Romesberg, F.E., 2006. Induction and inhibition of ciprofloxacin resistance-conferring mutations in hypermutator bacteria. Antimicrob. Agents Chemother. 50, 220–225. https://doi.org/10.1128/AAC.50.1.220-225.2006.

Cook, M.A., Wright, G.D., 2022. The past, present, and future of antibiotics. Sci. Transl. Med. https://doi.org/10.1126/scitranslmed.abo7793.

Crane, J.K., Alvarado, C.L., Sutton, M.D., 2021. Role of the SOS response in the generation of antibiotic resistance in vivo. Antimicrob. Agents Chemother. 65 https://doi.org/10.1128/AAC.00013-21.

Crooks, G.E., Hon, G., Chandonia, J.M., Brenner, S.E., 2004. WebLogo: a sequence logo generator. Genome Res 14, 1188–1190. https://doi.org/10.1101/gr.849004.

Culyba, M.J., Kubiak, J.M., Mo, C.Y., Goulian, M., Kohli, R.M., 2018. Non-equilibrium repressor binding kinetics link DNA damage dose to transcriptional timing within the SOS gene network. PLOS Genet 14, e1007405. https://doi.org/10.1371/journal.pgen.1007405.

Da Re, S., Garnier, F., Guérin, E., Campoy, S., Denis, F., Ploy, M.C., 2009. The SOS response promotes qnrB quinolone-resistance determinant expression. EMBO Rep. 10, 929–933. https://doi.org/10.1038/embor.2009.99.

Dajkovic, A., Mukherjee, A., Lutkenhaus, J., 2008. Investigation of regulation of FtsZ assembly by SulA and development of a model for FtsZ polymerization. J. Bacteriol. 190, 2513–2526. https://doi.org/10.1128/JB.01612-07.

Datsenko, K.A., Wanner, B.L., 2000. One-step inactivation of chromosomal genes in Escherichia coli K-12 using PCR products. Proc. Natl. Acad. Sci. 97, 6640–6645. https://doi.org/10.1073/pnas.120163297.

Davis, K.M., 2020. For the greater (Bacterial) good: heterogeneous expression of energetically costly virulence factors. Infect. Immun. 88 https://doi.org/10.1128/IAI.00911-19.

Davis, K.M., Isberg, R.R., 2016. Defining heterogeneity within bacterial populations via single cell approaches. BioEssays. https://doi.org/10.1002/bies.201500121.

Dörr, T., Vulić, M., Lewis, K., 2010. Ciprofloxacin causes persister formation by inducing the TisB toxin in Escherichia coli. PLoS Biol. 8 https://doi.org/10.1371/JOURNAL.PBIO.1000317.

Ducret, A., Quardokus, E.M., Brun, Y.V., 2016. MicrobeJ, a tool for high throughput bacterial cell detection and quantitative analysis. Nat. Microbiol. 1 (7), 1. https://doi.org/10.1038/nmicrobiol.2016.77.

Gouy, M., Tannier, E., Comte, N., Parsons, D.P., 2021. Seaview Version 5: a multiplatform software for multiple sequence alignment, molecular phylogenetic analyses, and tree reconciliation. : Methods Mol. Biol. Methods Mol. Biol. 241–260. https://doi.org/10.1007/978-1-0716-1036-7_15.

Hughes, D., Andersson, D.I., 2017. Environmental and genetic modulation of the phenotypic expression of antibiotic resistance. FEMS Microbiol. Rev. https://doi.org/10.1093/femsre/fux004.

Jaramillo-Riveri, S., Broughton, J., McVey, A., Pilizota, T., Scott, M., El Karoui, M., 2022. Growth-dependent heterogeneity in the DNA damage response in Escherichia coli. Mol. Syst. Biol. 18 https://doi.org/10.15252/msb.202110441.

Jones, E.C., Uphoff, S., 2021. Single-molecule imaging of LexA degradation in Escherichia coli elucidates regulatory mechanisms and heterogeneity of the SOS response. Nat. Microbiol. 6, 981–990. https://doi.org/10.1038/s41564-021-00930-y.

Katoh, K., Rozewicki, J., Yamada, K.D., 2018. MAFFT online service: multiple sequence alignment, interactive sequence choice and visualization. Brief. Bioinform. 20, 1160–1166. https://doi.org/10.1093/bib/bbx108.

Keseler, I.M., Gama-Castro, S., Mackie, A., Billington, R., Bonavides-Martínez, C., Caspi, R., Kothari, A., Krummenacker, M., Midford, P.E., Muñiz-Rascado, L., Ong, W. K., Paley, S., Santos-Zavaleta, A., Subhraveti, P., Tierrafría, V.H., Wolfe, A.J., Collado-Vides, J., Paulsen, I.T., Karp, P.D., 2021. The EcoCyc Database in 2021. Front. Microbiol. 12 https://doi.org/10.3389/fmicb.2021.711077.

Machuca, J., Recacha, E., Gallego-Mesa, B., Diaz-Diaz, S., Rojas-Granado, G., Garciá-Duque, A., Docobo-Pérez, F., Blázquez, J., Rodríguez-Rojas, A., Pascual, A., Rodríguez-Martínez, J.M., 2021. Effect of RecA inactivation on quinolone susceptibility and the evolution of resistance in clinical isolates of Escherichia coli. J. Antimicrob. Chemother. 76, 338–344. https://doi.org/10.1093/jac/dkaa448.

Maslowska, K.H., Makiela-Dzbenska, K., Fijalkowska, I.J., 2019. The SOS system: a complex and tightly regulated response to DNA damage. Environ. Mol. Mutagen. https://doi.org/10.1002/em.22267.

Mérida-floriano, A., Rowe, W.P.M., Casadesús, J., 2021. Genome-wide identification and expression analysis of sos response genes in salmonella enterica serovar typhimurium. Cells 10. https://doi.org/10.3390/cells10040943.

Overhage, J., Bains, M., Brazas, M.D., Hancock, R.E.W., 2008. Swarming of Pseudomonas aeruginosa is a complex adaptation leading to increased production of virulence factors and antibiotic resistance. J. Bacteriol. 190, 2671–2679. https://doi.org/10.1128/JB.01659-07.

Pribis, J.P., García-Villada, L., Zhai, Y., Lewin-Epstein, O., Wang, A.Z., Liu, J., Xia, J., Mei, Q., Fitzgerald, D.M., Bos, J., Austin, R.H., Herman, C., Bates, D., Hadany, L., Hastings, P.J., Rosenberg, S.M., 2019. Gamblers: an antibiotic-induced evolvable cell subpopulation differentiated by reactive-oxygen-induced general stress response. .e7 Mol. Cell 74, 785–800. https://doi.org/10.1016/J.MOLCEL.2019.02.037.

Recacha, E., Machuca, J., Díaz de Alba, P., Ramos-Güelfo, M., Docobo-Pérez, F., Rodriguez-Beltrán, J., Blázquez, J., Pascual, A., Rodríguez-Martínez, J.M.M., 2017. Quinolone resistance reversion by targeting the SOS response. MBio 8. https://doi.org/10.1128/mBio.00971-17.

Recacha, E., Machuca, J., Díaz-Díaz, S., García-Duque, A., Ramos-Guelfo, M., Docobo-Pérez, F., Blázquez, J., Pascual, A., Rodríguez-Martínez, J.M., 2019. Suppression of the SOS response modifies spatiotemporal evolution, post-antibiotic effect, bacterial fitness and biofilm formation in quinolone-resistant Escherichia coli. J. Antimicrob. Chemother. 74, 66–73. https://doi.org/10.1093/jac/dky407.

Rodríguez-Martínez, J.M., Machuca, J., Cano, M.E., Calvo, J., Martínez-Martínez, L., Pascual, A., 2016. Plasmid-mediated quinolone resistance: two decades on. Drug Resist. Updat. 29, 13–29. https://doi.org/10.1016/J.DRUP.2016.09.001.

Sánchez-Romero, M.A., Casadesús, J., 2014. Contribution of phenotypic heterogeneity to adaptive antibiotic resistance. Proc. Natl. Acad. Sci. U. S. A. 111, 355–360. https://doi.org/10.1073/pnas.1316084111.

Takhaveev, V., Heinemann, M., 2018. Metabolic heterogeneity in clonal microbial populations. Curr. Opin. Microbiol. 45, 30–38. https://doi.org/10.1016/J.MIB.2018.02.004.

Vincent, M.S., Uphoff, S., 2020. Bacterial phenotypic heterogeneity in DNA repair and mutagenesis. Biochem. Soc. Trans. https://doi.org/10.1042/BST20190364.

Zaslaver, A., Bren, A., Ronen, M., Itzkovitz, S., Kikoin, I., Shavit, S., Liebermeister, W., Surette, M.G., Alon, U., 2006. A comprehensive library of fluorescent transcriptional reporters for Escherichia coli. Nat. Methods 3, 623–628. https://doi.org/10.1038/nmeth895.